

# Cascade of transitions in twisted bilayer graphene – the Van Hove scenario

Dmitry V. Chichinadze,<sup>1</sup> Laura Classen,<sup>2</sup> Yuxuan Wang,<sup>3</sup> and Andrey V. Chubukov<sup>4,1</sup>

<sup>1</sup>*School of Physics and Astronomy, University of Minnesota, Minneapolis, MN 55455, USA*

<sup>2</sup>*Max Planck Institute for Solid State Research, D-70569 Stuttgart, Germany*

<sup>3</sup>*Department of Physics, University of Florida, Gainesville, Florida 32601*

<sup>4</sup>*W. I. Fine Theoretical Physics Institute, University of Minnesota, Minneapolis, Minnesota 55455, USA*

Measurements of compressibility in twisted bilayer graphene showed a cascade of phase transitions with increasing electron or hole filling  $n$ , and STM measurements showed that in a wide range of  $n$  one of the Van Hove peaks in the density of states remains close to the chemical potential. Motivated by these experiments, we analyze the pattern of spontaneous symmetry breakings for itinerant fermions near a Van Hove singularity. We make use of an approximate SU(4) symmetry of the manifold of spin/isospin (valley) orders, analyze the Landau free energy, and show that the structure of the spin/isospin order parameter changes with increasing  $|n|$  via a cascade of phase transitions. We compute the feedback from different spin/isospin orders on fermions and argue that each order splits the initially 4-fold degenerate Van Hove peak in a particular fashion, consistent with the STM data, and gives rise to a sharp change of compressibility, thus providing a unified interpretation of STM and compressibility data for twisted bilayer graphene. Our results follow from a generic analysis of an SU(4)-symmetric Landau functional and are valid beyond a specific fermionic model used to derive the functional.

**Introduction.** Twisted bilayer graphene (TBG) is a two-dimensional correlated electronic system, which exhibits superconductivity [1–3] and correlated phases [4–13]. The focus of our work is the analysis of a cascade of phase transitions near integer fillings  $|n| = 1, 2, 3, 4$ , detected in STM and electronic compressibility measurements [5, 14, 15] (panels (a)–(c) in Fig. 1). Compressibility measurements show sharp seesaw features of  $d\mu/dn$  near integer  $|n|$ , and STM data show that around each of these  $n$  a peak in the density of states splits, and one of its components appears on the other side of the Fermi level. For the interpretation, the authors of [14] adopted a strong coupling approach and associated the observed STM peaks with narrow sub-bands. They argued that at each transition one sub-band crosses the Fermi level, moves away from it, and becomes completely incoherent. The authors of [15] interpreted compressibility data within a moderate coupling scenario of a 4-fold spin/isospin degenerate band and argued that the cascade can be understood as a series of interaction-driven transitions. They conjectured that at, e.g., electronic doping one of the bands gets completely filled at each transition, while the occupation of the remaining ones gets depleted; mirror symmetric behavior holds for hole doping.

In this communication we propose the scenario in which the cascade of transitions is caused by the development of particle-hole orders, like in [15], but we specifically identify the STM peaks with Van Hove (VH) singularities. We argue that the electronic orders are of VH origin, and that the components of the initially 4-fold degenerate VH peak move through the Fermi level one by one, but remain close to it. The split peaks recombine into a single 4-fold peak at  $|n| \lesssim 4$ , when electronic order vanishes. Our scenario is summarized in panels (a1), (b1), and (d) in Fig. 1. For the justification of the moderate coupling VH-based approach, we note that VH peaks have been observed in TBG at dif-

ferent twisting angles [6, 16] and are present in the electronic dispersion obtained in first-principle calculations and in the ones renormalized by the interaction, even if the bottom of the dispersion moves away from Dirac points [17]. Also, the cascade of transitions has been observed in magic-angle twisted trilayer graphene [18] (and argued to be triggered by VH peaks, at least at high displacement fields) and in less correlated Bernal bilayer and rhombohedral trilayer graphene [19–21].

The summary of our results is presented in Fig. 1 along with the experimental data from Refs. [14, 15]. We label the VH peaks in conduction (valence) bands in by  $I$  ( $II$ ) and label peel components by  $a, b, c, d$ . Our interpretation of the STM data from Ref. [14] for electron doping (panel (a2)) is the following: as the system moves away from charge neutrality, the 4-fold degenerate peak  $I_{a+b+c+d}$  approaches  $\mu$  from above, and at  $n \leq 1$ , splits in a 3-1 fashion: three components  $I_{a+b+c}$  stay above  $\mu$ , and one component,  $I_d$ , jumps to below the Fermi level, but remains close to it. At  $n \leq 2$ , the three components again come close to  $\mu$ , and the VH peak  $I_{a+b+c}$  splits in 2-2 fashion, such that  $I_{a+b}$  moves back, while  $I_c$  jumps to below the Fermi level and merges with  $I_d$  into  $I_{c+d}$ . At  $n \leq 3$ ,  $I_{a+b}$  splits and  $I_b$  jumps to below the Fermi level and merges with  $I_{c+d}$  into  $I_{b+c+d}$ . Finally, at  $n \leq 4$ , the last component  $I_a$  jumps across the Fermi level and merges with three other components into 4-fold degenerate  $I_{a+b+c+d}$ . For hole doping the overall evolution is the same, but the data seem to show a more gradual behavior: the components of peak  $II$  in panel (b2) cross the Fermi level one-by-one, i.e., the sequence of splittings is  $3 - 1, 2 - 1 - 1, 1 - 2 - 1, 1 - 3$ .

We consider these data as evidence that once the 4-fold degenerate VH peak gets close to  $\mu$  at  $|n| \sim 1$  (peak  $I$  for  $n > 0$  and peak  $II$  for  $n < 0$ ), the system develops a VH-induced particle-hole order. The order exists between

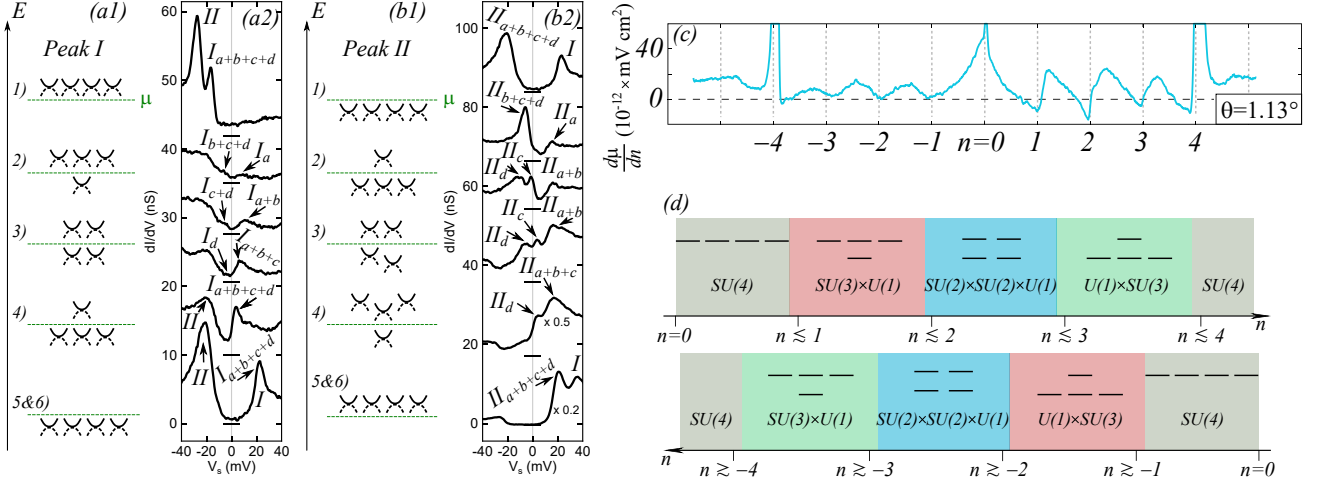


FIG. 1. The cascade of electronic transitions in twisted bilayer graphene. (a), (b): the proposed splitting of the initially 4-fold (spin and valley) degenerate VH peak upon raising the electron (a) and hole (b) filling  $n$  and the corresponding STM data for twist angle of  $1.06^\circ$ , reproduced with permission from the authors of Ref. [14]. The Van Hove peaks in the conduction (valence) bands are labeled by  $I$  ( $II$ ), and a,b,c,d label the 4 peak components. Saddle-point spectra in (a1), (b1) illustrate VH singularities. (c): experimental data for inverse compressibility with seesaw features, interpreted as a cascade of phase transitions. Reproduced with permission from the authors of Ref. [15]. The data are for twist angle  $\theta = 1.13^\circ$ , (d) The schematic phase diagram of TBG upon electron or hole doping, based on comparison between the theory and the STM data. Within our model, we obtained  $SU(3) \times U(1)$  ( $U(1) \times SU(3)$ ) symmetry for both electron and hole doping at  $1 < |n| < 2$  ( $3 < |n| < 4$ ), corresponding to 3-1 (1-3) splitting, but it is reduced to  $SU(2) \times U(1) \times U(1)$  ( $U(1) \times U(1) \times SU(2)$ ) if there is an intermediate phase with 2-1-1 (1-1-2) splitting, as STM data for hole doping likely indicate.

$|n| \lesssim 1$  and  $|n| \lesssim 4$  and reconstructs the fermionic spectra, pushing VH peaks in some bands to above  $\mu$  and in other band(s) to below  $\mu$ . The structure of the order changes near  $|n| = 2$  and  $|n| = 3$ , via first-order transitions, and this changes the splitting of the VH peak and simultaneously gives rise to sharp changes in the compressibility (see Fig. 1 (c)).

Here, we present the theoretical description of this scenario within the model of interacting itinerant electrons whose band structure has a VH singularity near  $\mu$ . We use as an input our earlier result [22, 23] that the increased density of states near the VH singularity enables a spontaneous symmetry breaking in spin and valley spaces. For a model with intra-site (Hubbard) and inter-site interactions within a given hexagon [24], we found 15 particle-hole order parameters, for which the couplings are attractive, near-equal, and larger than for other order parameters. These 15 order parameters are described by  $4 \times 4$  matrices in spin and valley spaces, specified by spin  $\sigma$  and valley isospin  $\tau$  and form the adjoint representation of the  $SU(4)$  group. For shortness, we call an order in  $(\sigma, \tau)$  space a spin/isospin order. An  $SU(4)$ -symmetric order parameter manifold and the interplay between spin and isospin orders have been recently discussed in [25–31] – these works provide additional motivation for us. Another input for our analysis are band structure calculations [32, 33] which reported the pinning of the VH singularity to the chemical potential over the range of

$n$ .

In Ref. [23] we analyzed the instabilities near VH doping neglecting cubic terms in the free energy. We found a certain degenerate manifold of ordered states, each giving rise to a  $2 \times 2$  splitting of the original VH peak into two doubly degenerate peaks. This is consistent with the data at  $|n| \gtrsim 2$ , but not at  $|n| \sim 1$  and  $|n| \gtrsim 3$ . To explain the phase transition near  $|n| = 1$  we entertained a possibility of a separate instability, developing when the VH peak is away from  $\mu$ , and conjectured that in between  $|n| = 1$  and  $|n| = 2$  the system goes back to a metallic state with four equally filled degenerate bands. In this work we verify whether one can explain the system's behavior at all relevant  $n$  within a single VH scenario, i.e., relate the cascade of phase transitions and splitting of VH peaks to the evolution of VH-induced particle-hole order. For this we analyze the full Landau free energy for an  $SU(4)$ -symmetric fermionic model, including the cubic terms in the order parameters. Our analysis is solely based on symmetry and remains valid beyond a particular microscopic model used to derive the free energy.

We find that the first VH-induced instability splits the 4-fold degenerate VH peak in a 3-1 fashion, with peaks for 3 degenerate bands shifting towards charge neutrality, and the remaining peak moving to below  $\mu$ . As the magnitude of a spin/isospin order increases, the system undergoes a transition into a different ordered state, which gives rise to 2-2 splitting of the VH peak. The transition is direct and first-

order in our model, but in reality may occur via an intermediate phase with 2-1-1 splitting. At  $|n| \sim 3$  the magnitude of the order starts decreasing as some of VH peak components move further away from  $\mu$ , and the system behavior goes in reverse - first the system undergoes a transition into an ordered state which gives rise to 1-3 VH peak splitting, again either via a direct first-order transition, or via an intermediate phase with 1-1-2 splitting, and then, at even larger  $|n| \leq 4$ , the order vanishes, and all 4 VH peak components merge into a single VH peak below  $\mu$ .

**Model** Band structure calculations show that there are eight bands within the flat-band regime of TBG, accounting for two spin projections, two valley degrees of freedom from the original graphene layers, and two sublattices of the moiré superlattice. Four bands are with upward and four with downward dispersion, merging at Dirac points  $K$  and  $K'$ . Upon electron (hole) doping the chemical potential moves up (down), simultaneously changing the filling of four bands. Each band displays a VH singularity. The VH singularities for four conduction (four valence) bands are at the same energy. It was argued that strong coupling renormalizations shift the minimum of electron band to the  $\Gamma$  point [17, 32], but VH singularities remain even for the renormalized dispersion [32, 34].

We study the cascade of phase transitions by analyzing the Landau free energy for the ordered phases of fermions with VH singularity near  $\mu$ . The order parameters are expectation values of fermionic bilinears, and the free energy can be obtained by integrating out fermions after performing a Hubbard-Stratonovich transformation associated with these bilinears. Alternatively, one can write down the Landau free energy solely based on symmetries and fix parameters phenomenologically through comparison with experiments. In an earlier study [23] we found that out of a large number of possible fermionic bilinears (143 in the 6-patch VH model and even larger number in 12-patch model) there are 15, for which the couplings are attractive and the largest by magnitude. The set of 15 is composed of two subsets of 7 and 8 bilinears with a single coupling within each subset ( $\lambda_7$  and  $\lambda_8$ , respectively; 7 bilinears are intra-valley with transferred momentum  $Q = 0$ , 8 are inter-valley with a finite  $Q$ ). The couplings  $\lambda_7$  and  $\lambda_8$  are not identical, but are close to each other. In our analysis we treat  $\lambda_7$  and  $\lambda_8$  as equal, in which case the 15 bilinears form an adjoint representation of  $SU(4)$ . We checked that the cascade of transitions and the sequence of VH peak splitting is the same in the model with only 7 bilinears (the case  $\lambda_7 > \lambda_8$ ). In the model with 8 bilinears there is a single ordered phase and no cascade.

For the  $SU(4)$  case, the Landau free energy up to fourth order is [23] [35]

$$\mathcal{F} = -\frac{\alpha}{2}\text{Tr}[\hat{\Phi}^2] + \frac{\gamma}{3}\text{Tr}[\hat{\Phi}^3] + \frac{\beta}{4}\text{Tr}[\hat{\Phi}^4] + \frac{\beta'}{4}\text{Tr}[\hat{\Phi}^2]^2, \quad (1)$$

where  $\hat{\Phi} = \sum_{j=1}^{15} \phi_j T^j$ ,  $T^j$  are generators of  $SU(4)$ , and  $\phi_j \sim f^\dagger T^j f$  are fermionic bilinears, which we treat as

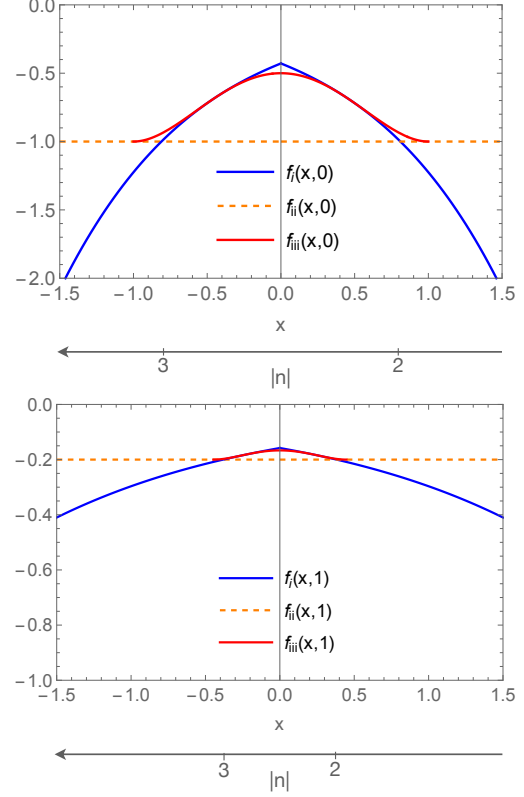


FIG. 2. The functions  $f_l(x, y)$  from Eq. (4), with  $l = i, ii, iii$ , shown as functions of  $x = \gamma / \sqrt{\alpha\beta}$  for two values of  $y = \beta' / \beta$ :  $y = 0$  and  $y = 1$ . The free energies are  $F_l = (\alpha^2 / \beta) f_l(x, y)$ , hence the smallest  $f_l(x, y)$  determines the ground state. The states (i) and (ii) are the ones for which the VH peaks split in 3-1 (1-3) and 2-2 fashion, respectively. The state (iii) is an intermediate state with 2-1-1 (1-1-2) splitting. This intermediate state does not appear as a ground state in our model for all  $y$ , but its energy is close to those of (i) and (ii) near critical  $x$  of the first-order transition between the two, and it can potentially become a ground state around this  $x$  if we move away from  $SU(4)$ -symmetric model by e.g., including interaction terms with inter-valley scattering. The relation between  $x$  and  $|n|$  is shown at the bottom.

Hubbard-Stratonovich fields ( $f$  and  $f^{(\dagger)}$  are operators of electrons near VH points). The term  $\beta'$  does not appear within Hubbard-Stratonovich but is allowed by symmetry, and we keep it for generality.

By construction,  $\hat{\Phi}$  can be represented by a traceless matrix [36]. In the diagonal basis

$$\hat{\Phi} = \text{diag}(\lambda_1, \lambda_2, \lambda_3, -(\lambda_1 + \lambda_2 + \lambda_3)), \quad (2)$$

and the free energy is

$$\mathcal{F} = -\frac{\alpha}{2} \left( \sum_j^3 \lambda_j^2 + \left( \sum_j^3 \lambda_j \right)^2 \right) + \frac{\gamma}{3} \left( \sum_j^3 \lambda_j^3 - \left( \sum_j^3 \lambda_j \right)^3 \right) + \frac{\beta}{4} \left( \sum_j^3 \lambda_j^4 + \left( \sum_j^3 \lambda_j \right)^4 \right) + \frac{\beta'}{4} \left( \sum_j^3 \lambda_j^2 + \left( \sum_j^3 \lambda_j \right)^2 \right)^2. \quad (3)$$

At  $\gamma = 0$ , the order develops continuously when  $\alpha$  changes sign and becomes positive. At a finite  $\gamma$ , the transition is necessarily first order and occurs already when  $\alpha$  is negative. Below we restrict to  $\alpha > 0$ , when the order is already finite and also set  $\beta > 0$ , consistent with the Hubbard-Stratonovich analysis for the tight-binding model near a VH singularity [23]. Minimizing  $\mathcal{F}$  with respect to  $\lambda_j$  ( $j = 1, 2, 3$ ), we find three solutions, up to permutations of  $\lambda_j$ : (i)  $\lambda_1 = \lambda_2 = \lambda_3$ ; (ii)  $\lambda_1 = \lambda_2 = -\lambda_3$ ; (iii)  $\lambda_1 = \lambda_2 \neq \lambda_3$  (see Supplementary material (SM) for details). For the first solution,  $\hat{\Phi} = \text{diag}(\lambda, \lambda, \lambda, -3\lambda)$ , and the broken symmetry is described by the coset  $\text{SU}(4)/[\text{SU}(3) \times \text{U}(1)]$ , where  $\text{SU}(3)$  corresponds to the transformation within the subset of the first three components of  $\hat{\Phi}$ , and  $\text{U}(1)$  to a rotation of the last component relative to the other three. The ordered

states in terms of expectation values of fermionic bilinears  $\langle \phi_i \rangle$  are mixtures of spin/isospin order with particular ratios of spin and isospin components [23]. For example, a pure intra-valley order is a part of this set, but a pure inter-valley order is not. The order parameter manifold has  $15 - 8 - 1 = 6$  Goldstone modes. The feedback of this order on fermions is 3-1 or 1-3 splitting of VH peaks, depending on the sign of  $\gamma$ . For the second solution,  $\hat{\Phi} = \text{diag}(\lambda, \lambda, -\lambda, -\lambda)$ , and the broken symmetry is  $\text{SU}(4)/[\text{SU}(2) \times \text{SU}(2) \times \text{U}(1)]$ , where the two  $\text{SU}(2)$ 's correspond to rotations within the subsets of the first two and the last two components of  $\hat{\Phi}$ , and  $\text{U}(1)$  corresponds to a rotation of one subset relative to the other. The ordered states in terms of  $\langle \phi_i \rangle$  include pure spin and isospin orders, e.g. intra-valley ferromagnetism and valley polarization, and various inter-valley density waves [23]. This manifold has  $15 - 6 - 1 = 8$  Goldstone modes. The feedback from such order on fermions leads to 2-2 splitting of the VH peaks. Finally, the third solution describes a mixed state with  $\hat{\Phi} = \text{diag}(\lambda, \lambda, -\lambda_3, -2\lambda + \lambda_3)$  and broken symmetry  $\text{SU}(4)/[\text{SU}(2) \times \text{U}(1) \times \text{U}(1)]$ . The order parameter manifold contains  $15 - 3 - 1 - 1 = 10$  Goldstone modes. The feedback on fermions leads to 2-1-1 or 1-1-2 splitting of VH peaks.

The values of  $\lambda$  and the free energies for the three states,  $F_i = \frac{\alpha^2}{\beta} f_i(x, y)$ , are functions of  $x = \gamma / \sqrt{\alpha\beta}$  and  $y = \beta' / \beta$ :

$$\begin{aligned} \text{(i)} \lambda_i &= \sqrt{\frac{\alpha}{\beta}} \frac{|x| \pm \sqrt{x^2 + 7 + 12y}}{7 + 12y}, \quad f_i(x, y) = -\frac{(|x| \pm \sqrt{7 + x^2 + 12y})^2 [3(7 + 12y) + 2|x|(|x| \pm \sqrt{7 + x^2 + 12y})]}{(7 + 12y)^3} \\ \text{(ii)} \lambda_{ii} &= \sqrt{\frac{\alpha}{\beta}} \frac{1}{\sqrt{1 + 4y}}, \quad f_{ii}(x, y) = -\frac{1}{1 + 4y} \\ \text{(iii)} \lambda_{iii} &= \sqrt{\frac{\alpha}{\beta}} x, \quad \lambda_{iii,3} = \sqrt{\frac{\alpha}{\beta}} \left( \sqrt{\frac{1 - x^2(1 + 4y)}{1 + 2y}} - |x| \right), \quad f_{iii}(x, y) = -\frac{1 + 2x^2 - x^4(1 + 4y)}{2(1 + 2y)}. \end{aligned} \quad (4)$$

The solution (iii) exists for  $|x| \leq 1 / \sqrt{1 + 4y}$  and the  $\pm$  sign is for positive/negative  $\gamma$ . We plot the free energy prefactors  $f_i(x, y)$  in Fig. 2.

We see that at large  $|x|$  the ground state configuration is state (i) while for small  $|x|$  it is state (ii). There is a direct first-order transition between states (i) and (ii) at some intermediate  $|x| = x_{cr}$ . We expect that  $\alpha > 0$  between  $1 < |n| < 4$ , where the VH peak remains near the chemical potential, and conjecture that  $\gamma$  changes sign from positive to negative as  $|n|$  increases, as the sign of  $\gamma$  is different when the bands are empty and when they are filled. As a result  $x$  evolves from a large positive value to a large negative one via zero upon increasing  $|n|$ . Because small  $\alpha$  corresponds to large  $|x|$ , when the order first emerges, the system moves into state (i), and the components of the VH peak split in 1-3 fashion for positive  $\gamma$ . As  $\alpha$  increases,  $|x|$  decreases and eventually

reaches  $x_{cr}$ , where the system undergoes a first order transition into the ordered state (ii), for which the splitting of the components of the VH peak is 2-2. At larger  $n$ ,  $\gamma$  changes sign and its magnitude increases, while  $\alpha$  starts decreasing. As a result,  $|x|$  increases. When it reaches  $x_{cr}$ , the system undergoes another first-order transition into the state, which gives rise to 3-1 splitting of the components of the VH peak. Eventually the order disappears and all 4 components of the VH peak recombine into a single peak. We also note that while the intermediate state (iii) is not the ground state for any  $x$  and  $y$ , its free energy  $F_{iii}$  is only slightly larger than  $F_i$  and  $F_{ii}$  at  $|x|$  near  $x_{cr}$ . This is particularly so at large  $y$  (at  $x_{cr} \approx \sqrt{3/16y}$ ,  $F_{iii}$  is larger than  $F_i = F_{ii}$  by  $(\alpha^2/\beta)1/(16y)^2$ ). Thus, it seems possible that the intermediate state (iii) will become the ground state once we move away from an  $\text{SU}(4)$ -symmetric model by e.g., including in-

teraction terms with inter-valley scattering. Such terms are small, but finite in TBG [24, 37, 38]. If the transition from (i) to (ii) is via the intermediate phase (iii), there is a range of  $|n|$  where the splitting of the VH peak components is 2-1-1 or 1-1-2, again depending on the sign of  $\gamma$ . Signatures of 2-1-1 and 1-1-2 splitting have indeed been found in STM for hole-doped samples.

**Comparison with experiments.** In our proposed VH scenario, spin/isospin order develops at  $|n| \lesssim 1$ , when the four-fold degenerate VH peak approaches the Fermi level, and persists up to  $|n| \lesssim 4$ . In this range of  $n$ , the VH peak splits, but according to STM data, its components are still located near the Fermi energy, i.e., the enhancement of the DOS near the Fermi level persists. At larger  $|n|$ , the VH peak again becomes four-fold degenerate and moves away from the Fermi level. The evolution of spin/isospin order and of its feedback on the components of the VH peak is governed in our theory by the relative strength of the prefactor of the cubic term in the Landau free energy (specifically, by  $x = \gamma/\sqrt{\alpha\beta}$ ). This prefactor is expressed via a convolution of three fermionic propagators and vanishes for particle-hole symmetry around the Fermi surface. In the absence of such symmetry,  $\gamma$  is non-zero. We conjecture that  $x$  is positive near  $n = 1$  passes through zero at  $2 < n < 3$ , and becomes negative at larger  $n$ . We then end up with the phase diagram in Fig. 1 (d). There are two phase transitions between disordered and ordered states at  $|n| \lesssim 1$ , and  $|n| \lesssim 4$ , and two transitions between different ordered phases at  $|n| \lesssim 2$  and  $|n| \lesssim 3$ . Specifically, within our theory the sequence for the symmetry-breaking pattern and the degeneracy of the VH peak is:

$$\begin{aligned} n \lesssim 1: & \text{SU}(4) \rightarrow \text{SU}(3) \times \text{U}(1) : (4, 0) \rightarrow (3, 1) \\ n \lesssim 2: & \text{SU}(3) \times \text{U}(1) \rightarrow \text{SU}(2) \times \text{SU}(2) \times \text{U}(1) : (3, 1) \rightarrow (2, 2) \\ n \lesssim 3: & \text{SU}(2) \times \text{SU}(2) \times \text{U}(1) \rightarrow \text{U}(1) \times \text{SU}(3) : (2, 2) \rightarrow (1, 3) \\ n \lesssim 4: & \text{U}(1) \times \text{SU}(3) \rightarrow \text{SU}(4) : (1, 3) \rightarrow (0, 4) \end{aligned} \quad (5)$$

where  $a$  and  $b$  in  $(a, b)$  indicate the number of VH peaks above and below  $\mu$  for the case of electron doping. For hole doping the sequence is identical, except  $a$  and  $b$  in  $(a, b)$  are interchanged. If the transformations  $(3, 1) \rightarrow (2, 2)$  and  $(2, 2) \rightarrow (1, 3)$  occur via an intermediate phase (c), each of the two first-order transitions around  $|n| = 2$  is replaced by two second-order transitions with the intermediate structure of VH peaks  $(2, 1, 1)$  and  $(1, 1, 2)$ .

The theoretical phase diagram agrees with the STM results [5, 14] (Fig. 1 (a2,b2)), including fine details, lending support to our theory. Note, that there is no symmetry of the phase diagram with respect to  $|n| = 2$ , i.e. the transitions at  $|n| \lesssim 1$  and  $n \lesssim 3$  are different ones (there is an approximate symmetry with respect to  $|n| = 2.5$ ). The theory also explains the seesaw behavior of electron compressibility, reported in [15] and shown in Fig. 1 (c). Within our approach the regions where inverse compressibility has a negative (positive) slope for electron (hole) doping are as-

sociated with the phases between transitions, i.e. the SU(4)-symmetric phase at  $|n| \lesssim 1$ , the ordered states with residual SU(3)  $\times$  U(1) symmetry between  $|n| \lesssim 1$  and  $|n| \lesssim 2$  and between  $|n| \lesssim 3$  and  $|n| \lesssim 4$ , and the ordered state with residual SU(2)  $\times$  SU(2)  $\times$  U(1) symmetry at  $2 \lesssim |n| \lesssim 3$ . The regions with a positive (negative) slope correspond either to a broadened first-order transition or to the intermediate phase.

**Conclusions.** In this theoretical work, we used as an input STM data for TBG, which show that upon electron or hole doping, one of the VH peaks in the DOS remains near the chemical potential in a wide range of fillings – between  $|n| \lesssim 1$  and  $|n| \lesssim 4$ . We analyzed a cascade of phase transitions imposed by evolving spin/isospin order, which in turn is associated with the enhancement of the DOS for low-energy fermions due to a confinement of a VH peak close to  $\mu$ . We found a set of phase transitions: two first order transitions at  $|n| \lesssim 1$  and  $|n| \lesssim 4$  between disordered and ordered states and two transitions at  $|n| \lesssim 2$  and  $|n| \lesssim 3$  between different ordered states with different spin/isospin order and different splitting of VH peaks. These last transitions can be first order or continuous, via an intermediate phase. We argue that these transitions give rise to the seesaw behavior of the compressibility.

The semi-phenomenological explanation of the cascade of transitions put forward in Ref. [15] assumes that at every transition one of 4 initially degenerate bands gets fully filled/fully emptied and no longer contributes to particle-hole order. For our model, this would imply that each time a VH peak approaches  $\mu$  from above, a new component of spin/isospin order develops, and the original SU(4) symmetry transforms into SU(3)  $\times$  U(1), then into SU(2)  $\times$  U(1)  $\times$  U(1), and then into U(1)  $\times$  U(1)  $\times$  U(1). At each transition, the  $m$ -fold degenerate VH peak ( $m = 4, 3, 2$ ) splits into  $(m - 1, 1)$ . Within this scenario, one can naturally explain the emergence of insulating states at integer fillings, but one would need to explain why the four VH peaks, seemingly moving to different energies as  $|n|$  increases, recombine into a single VH peak at  $|n| \lesssim 4$ , as STM data show. We discuss this scenario in some detail in the SM. Interestingly, it yields the same ordered states as in our SU(4) scenario.

There is an element of phenomenology in our approach as well. Namely, we departed from a metal, associated the emergence of spin/isospin order with a VH singularity, and associated the cascade of transitions with near-integer  $|n|$  based on STM data rather than on microscopic calculations. The confinement of transitions to integer  $|n|$  and the emergence of insulating phases around these  $|n|$  are most likely strong-coupling phenomena. We note in this regard that the SU(4)-symmetric Landau free energy, on which our results and the results of Ref. [15] are based upon, is in fact generic, and while we derived it from the specific microscopic itinerant model of interacting fermions with  $\mu$  near the VH singularity, the same expression can be obtained

in a strong coupling limit, where the bands are assumed to be nearly completely flat [15, 17, 39–42], and their internal structure does not play a role. Within the strong-coupling scenario, the STM peaks, which we interpreted as Van Hove peaks, are treated as the peaks corresponding to flat bands. In either scenario, the Luttinger theorem states that the splitting due to spin/isospin orders can lead to the formation of insulating states only at integer fillings. In a recent experimental study [43] the authors argued that the cascade of transitions in TBG is present in a range of twist angles, even when there are no insulating states near integer fillings. These results lend further support to our Van Hove-based scenario of the cascade of phase transitions in

TBG.

**Acknowledgments.** We thank E. Berg, A. Cherman, Z. Dong, R. Fernandes, J. Hoffman, S. Ilani, P. Jarillo-Herrero, E. König, L. Levitov, Y. Oreg, H. Polshyn, G. Tarnopolsky, O. Vafek, A. Vishwanath, A. Yazdani, and E. Zeldov for fruitful discussions. We are indebted to S. Ilani, K. Nuckolls, A. Yazdani, and U. Zondiner for sharing their data with us. The work by D.V.C and A.V.C. was supported by U.S. Department of Energy, Office of Science, Basic Energy Sciences, under Award No. DE-SC0014402. Y.W. was supported by NSF under award number DMR-2045871. D.V.C. gratefully acknowledges support from Doctoral Dissertation and Larkin Fellowships at the University of Minnesota.

- 
- [1] Y. Cao, V. Fatemi, S. Fang, K. Watanabe, T. Taniguchi, E. Kaxiras, and P. Jarillo-Herrero, *Nature* **556**, 43 (2018).
- [2] M. Yankowitz, S. Chen, H. Polshyn, Y. Zhang, K. Watanabe, T. Taniguchi, D. Graf, A. F. Young, and C. R. Dean, *Science* **363**, 1059 (2019), <https://www.science.org/doi/pdf/10.1126/science.aav1910>.
- [3] Y. Cao, D. Rodan-Legrain, J. M. Park, N. F. Q. Yuan, K. Watanabe, T. Taniguchi, R. M. Fernandes, L. Fu, and P. Jarillo-Herrero, *Science* **372**, 264 (2021), <https://www.science.org/doi/pdf/10.1126/science.abc2836>.
- [4] Y. Cao, V. Fatemi, A. Demir, S. Fang, S. L. Tomarken, J. Y. Luo, J. D. Sanchez-Yamagishi, K. Watanabe, T. Taniguchi, E. Kaxiras, R. C. Ashoori, and P. Jarillo-Herrero, *Nature* **556**, 80 (2018).
- [5] Y. Xie, B. Lian, B. Jäck, X. Liu, C.-L. Chiu, K. Watanabe, T. Taniguchi, B. A. Bernevig, and A. Yazdani, *Nature* **572**, 101 (2019).
- [6] Y. Jiang, X. Lai, K. Watanabe, T. Taniguchi, K. Haule, J. Mao, and E. Y. Andrei, *Nature* **573**, 91 (2019).
- [7] G. Chen, A. L. Sharpe, E. J. Fox, Y.-H. Zhang, S. Wang, L. Jiang, B. Lyu, H. Li, K. Watanabe, T. Taniguchi, Z. Shi, T. Senthil, D. Goldhaber-Gordon, Y. Zhang, and F. Wang, *Nature* **579**, 56 (2020).
- [8] Y. Saito, J. Ge, L. Rademaker, K. Watanabe, T. Taniguchi, D. A. Abanin, and A. F. Young, *Nature Physics* **17**, 478 (2021).
- [9] Y. Xie, A. T. Pierce, J. M. Park, D. E. Parker, E. Khalaf, P. Ledwith, Y. Cao, S. H. Lee, S. Chen, P. R. Forrester, K. Watanabe, T. Taniguchi, A. Vishwanath, P. Jarillo-Herrero, and A. Yacoby, *Nature* **600**, 439 (2021).
- [10] A. L. Sharpe, E. J. Fox, A. W. Barnard, J. Finney, K. Watanabe, T. Taniguchi, M. A. Kastner, and D. Goldhaber-Gordon, *Science* **365**, 605 (2019), <https://www.science.org/doi/pdf/10.1126/science.aaw3780>.
- [11] M. Serlin, C. L. Tschirhart, H. Polshyn, Y. Zhang, J. Zhu, K. Watanabe, T. Taniguchi, L. Balents, and A. F. Young, *Science* **367**, 900 (2020), <https://www.science.org/doi/pdf/10.1126/science.aay5533>.
- [12] A. L. Sharpe, E. J. Fox, A. W. Barnard, J. Finney, K. Watanabe, T. Taniguchi, M. A. Kastner, and D. Goldhaber-Gordon, *Nano Letters* **21**, 4299 (2021).
- [13] C. L. Tschirhart, M. Serlin, H. Polshyn, A. Shragai, Z. Xia, J. Zhu, Y. Zhang, K. Watanabe, T. Taniguchi, M. E. Huber, and A. F. Young, *Science* **372**, 1323 (2021), <https://www.science.org/doi/pdf/10.1126/science.abd3190>.
- [14] D. Wong, K. P. Nuckolls, M. Oh, B. Lian, Y. Xie, S. Jeon, K. Watanabe, T. Taniguchi, B. A. Bernevig, and A. Yazdani, *Nature* **582**, 198 (2020).
- [15] U. Zondiner, A. Rozen, D. Rodan-Legrain, Y. Cao, R. Queiroz, T. Taniguchi, K. Watanabe, Y. Oreg, F. von Oppen, A. Stern, E. Berg, P. Jarillo-Herrero, and S. Ilani, *Nature* **582**, 203 (2020).
- [16] G. Li, A. Luican, J. M. B. Lopes dos Santos, A. H. Castro Neto, A. Reina, J. Kong, and E. Y. Andrei, *Nature Physics* **6**, 109 (2010).
- [17] J. Kang, B. A. Bernevig, and O. Vafek, *Phys. Rev. Lett.* **127**, 266402 (2021).
- [18] J. M. Park, Y. Cao, K. Watanabe, T. Taniguchi, and P. Jarillo-Herrero, *Nature* **590**, 249 (2021).
- [19] H. Zhou, L. Holleis, Y. Saito, L. Cohen, W. Huynh, C. L. Patterson, F. Yang, T. Taniguchi, K. Watanabe, and A. F. Young, *Science* **375**, 774 (2022), <https://www.science.org/doi/pdf/10.1126/science.abm8386>.
- [20] H. Zhou, T. Xie, T. Taniguchi, K. Watanabe, and A. F. Young, *Nature* **598**, 434 (2021).
- [21] H. Zhou, T. Xie, A. Ghazaryan, T. Holder, J. R. Ehrets, E. M. Spanton, T. Taniguchi, K. Watanabe, E. Berg, M. Serbyn, and A. F. Young, *Nature* **598**, 429 (2021).
- [22] D. V. Chichinadze, L. Classen, and A. V. Chubukov, *Phys. Rev. B* **102**, 125120 (2020).
- [23] D. V. Chichinadze, L. Classen, Y. Wang, and A. V. Chubukov, *Phys. Rev. Lett.* **128**, 227601 (2022).
- [24] J. Kang and O. Vafek, *Phys. Rev. Lett.* **122**, 246401 (2019).
- [25] Y. Wang, J. Kang, and R. M. Fernandes, *Phys. Rev. B* **103**, 024506 (2021).
- [26] N. Bultinck, E. Khalaf, S. Liu, S. Chatterjee, A. Vishwanath, and M. P. Zaletel, *Phys. Rev. X* **10**, 031034 (2020).
- [27] C. Xu and L. Balents, *Phys. Rev. Lett.* **121**, 087001 (2018).
- [28] J. W. F. Venderbos and R. M. Fernandes, *Phys. Rev. B* **98**, 245103 (2018).
- [29] J. Kang and O. Vafek, *Phys. Rev. Lett.* **122**, 246401 (2019).
- [30] L. Classen, C. Honerkamp, and M. M. Scherer, *Phys. Rev. B* **99**, 195120 (2019).
- [31] W. M. H. Natori, R. Nutakki, R. G. Pereira, and E. C. An-

- drade, Phys. Rev. B **100**, 205131 (2019).
- [32] T. Cea, N. R. Walet, and F. Guinea, Phys. Rev. B **100**, 205113 (2019).
- [33] L. Rademaker, D. A. Abanin, and P. Mellado, Phys. Rev. B **100**, 205114 (2019).
- [34] F. Guinea and N. R. Walet, Proceedings of the National Academy of Sciences **115**, 13174 (2018), <https://www.pnas.org/doi/pdf/10.1073/pnas.1810947115>.
- [35] Note, that the expression here uses a slightly different definition of prefactors in the free energy than the one in [23].
- [36] M. Hamermesh, Group theory and its application to physical problems (Courier Corporation, 2012).
- [37] J. Kang and O. Vafek, Phys. Rev. X **8**, 031088 (2018).
- [38] N. F. Q. Yuan and L. Fu, Phys. Rev. B **98**, 045103 (2018).
- [39] O. Vafek and J. Kang, Phys. Rev. Lett. **125**, 257602 (2020).
- [40] E. Khalaf, N. Bultinck, A. Vishwanath, and M. P. Zaletel, Soft modes in magic angle twisted bilayer graphene (2020).
- [41] B. Lian, Z.-D. Song, N. Regnault, D. K. Efetov, A. Yazdani, and B. A. Bernevig, Phys. Rev. B **103**, 205414 (2021).
- [42] P. J. Ledwith, E. Khalaf, and A. Vishwanath, Annals of Physics **435**, 168646 (2021), special issue on Philip W. Anderson.
- [43] R. Polski, Y. Zhang, Y. Peng, H. S. Arora, Y. Choi, H. Kim, K. Watanabe, T. Taniguchi, G. Refael, F. von Oppen, and S. Nadj-Perge, Hierarchy of symmetry breaking correlated phases in twisted bilayer graphene (2022).
- [44] N. Chen, T. A. Ryttov, and R. Shrock, Phys. Rev. D **82**, 116006 (2010).
- [45] S. Wu, Z. Zhang, K. Watanabe, T. Taniguchi, and E. Y. Andrei, Nature Materials **20**, 488 (2021).

## Supplemental Material

### S1. THE GROUND STATE OF THE SU(N) MODEL FOR N=4 AND N=3

In the main text we discuss an effective model of fermions near six (or twelve) Van Hove points in twisted bilayer graphene (TBG). The model consists of 4 sets of interacting fermions (2 spin and 2 valley isospin variables). We argued previously [23] that in both cases (six or twelve Van Hove points) there are 15 particle-hole order parameters (bilinear combinations of fermions) with nearly equal attractive couplings. The couplings for other order parameters are either repulsive or smaller by magnitude. More precisely, the set of 15 consists of two subsets of 7 and 8 bilinears. The couplings within each subset are identical ( $\lambda_7$  for the first subset,  $\lambda_8$  for the second). The couplings  $\lambda_7$  and  $\lambda_8$  are not identical, but are close to each other, and in our analysis we treated them as equal. These 15 fermionic bilinears then form an adjoint representation of the SU(4) group. Here we analyze in some detail the Landau free energy of the corresponding SU(4) model and obtain the structure of the ordered state for different parameters. For completeness, we also analyze the structure of the order in SU(N) models with  $N = 3$ , which in our case are effective models of fermions with 3 degenerate bands and  $N^2 - 1 = 8$  particle-hole bilinears with equal couplings (see Sec. S2 below). It is convenient to consider the general SU(N) case for the free energy and specify  $N = 4$  or  $N = 3$  in the next section.

The free energy of a system of  $N^2 - 1$  degenerate particle-hole order parameters  $\phi_i$  is, to fourth order in  $\phi_i$

$$\mathcal{F} = -\frac{\alpha}{2}\text{Tr}[\hat{\Phi}^2] + \frac{\gamma}{3}\text{Tr}[\hat{\Phi}^3] + \frac{\beta}{4}\text{Tr}[\hat{\Phi}^4] + \frac{\beta'}{4}\text{Tr}[\hat{\Phi}^2]^2. \quad (\text{S1})$$

Here  $\hat{\Phi} = \sum_j^{N^2-1} \phi_j T^j$ , where  $T^j$  are the generators of the group SU(N). Note, that the prefactors in the free energy are defined in a slightly different way than in [23]. The order-parameter fields  $\phi_j$  are expressed via fermionic bilinears as

$$\phi_j \sim f^\dagger T^j f \quad (\text{S2})$$

where  $f^\dagger$  and  $f$  are electronic creation and annihilation operators. The momentum-transfer between electrons can be zero or finite depending on which order  $\phi_j$  corresponds to.

This effective model can be straightforwardly obtained by departing from the Hamiltonian for  $N$  species with equal dispersion and 4-fermion interactions, selecting  $N^2 - 1$  particle-hole bilinears, applying a Hubbard-Stratonovich transformation, and integrating out the fermions. Note that in the effective model we considered previously [23], the dispersion of all fermion species was non-degenerate for different valleys so that the SU(4) symmetry was only approximate. The  $\beta'$ -term in (S1) does not appear in the ex-

pansion of the logarithm in the Hubbard-Stratonovich formalism, but is allowed on general grounds and in practice is generated in the renormalization group flow [44]. This term and the  $\beta$  term are the two independent quartic terms for  $N = 4$ . For  $N = 3$ ,  $\text{Tr}[\hat{\Phi}^2]^2 = 2\text{Tr}[\hat{\Phi}^4]$ , in which case the two terms are equivalent and we can  $\beta'$  into  $\beta$ .

In the Hubbard-Stratonovich formalism the sign of  $\gamma$  is determined by the sign of a one-loop diagram with three fermion-boson vertices and three propagators of low-energy fermions. The diagram vanishes in the limit when there is a particle-hole symmetry around the Fermi surface, but is non-zero in a generic case. For definiteness, below we set  $\gamma > 0$ . The extension to the case  $\gamma < 0$  changes the overall sign of the order parameter.

Because  $\hat{\Phi}$  is in the adjoint representation of the SU(N) group, it can be represented by a traceless matrix [36]. It is convenient to apply a unitary transformation and analyze  $\hat{\Phi}$  in the diagonal basis, where it takes the form

$$\hat{\Phi} = \text{diag}(\lambda_1, \lambda_2, \dots, \lambda_{N-1}, -(\lambda_1 + \dots + \lambda_{N-1})). \quad (\text{S3})$$

In this representation the free energy (S1) reads

$$\begin{aligned} \mathcal{F} = & -\frac{\alpha}{2} \left( \sum_j^{N-1} \lambda_j^2 + \left( \sum_j^{N-1} \lambda_j \right)^2 \right) + \frac{\gamma}{3} \left( \sum_j^{N-1} \lambda_j^3 - \left( \sum_j^{N-1} \lambda_j \right)^3 \right) \\ & + \frac{\beta}{4} \left( \sum_j^{N-1} \lambda_j^4 + \left( \sum_j^{N-1} \lambda_j \right)^4 \right) + \frac{\beta'}{4} \left( \sum_j^{N-1} \lambda_j^2 + \left( \sum_j^{N-1} \lambda_j \right)^2 \right)^2. \end{aligned} \quad (\text{S4})$$

Note that the first three terms in (S4) have the form of

$$\frac{\varkappa_n}{n} \left( \sum_j^{N-1} \lambda_j^n + (-1)^n \left( \sum_j^{N-1} \lambda_j \right)^n \right), \quad (\text{S5})$$

where  $\varkappa_n \in \{\alpha, \beta, \gamma\}$ . Below we explicitly minimize the free energy (S4) for  $N = 4, 3, 2$ . For definiteness we assume that the prefactor  $\alpha$  in (S4) is positive and analyze energy minimization for finite  $\lambda_j$ . The combination of stationary non-zero  $\lambda_j$  determines the type of order in terms of fermion bilinears  $\phi_j \sim \langle f^\dagger T^j f \rangle$  and also determines the shift of the Van Hove peaks of reconstructed energy bands.

#### A. The ground state of an SU(4)-symmetric free energy

For  $N = 4$  the order parameter matrix  $\hat{\Phi}$  in the diagonal basis is

$$\hat{\Phi} = \text{diag}(\lambda_1, \lambda_2, \lambda_3, -(\lambda_1 + \lambda_2 + \lambda_3)). \quad (\text{S6})$$

The free energy (S4) is then a function of three parameters  $\lambda_{1,2,3}$ . The values of these parameters are determined by the condition that the free energy is at a minimum. We analyze the solutions of  $\frac{\partial \mathcal{F}}{\partial \lambda_i} = 0$ . In explicit form

$$\frac{\partial F}{\partial \lambda_l} = -\alpha \left( \lambda_l + \sum_j \lambda_j \right) + \gamma \left[ \lambda_l^2 - \left( \sum_j \lambda_j \right)^2 \right] + \beta \left[ \lambda_l^3 + \left( \sum_j \lambda_j \right)^3 \right] + \beta' \left[ \sum_j \lambda_j^2 + \left( \sum_j \lambda_j \right)^2 \right] \left( \lambda_l + \sum_k \lambda_k \right) = 0 \quad (S7)$$

In our previous work [23] we set  $\gamma = \beta' = 0$  and found two solutions:  $\lambda_1 = \lambda_2 = -\lambda_3 = (\alpha/\beta)^{1/2}$  and  $\lambda_1 = \lambda_2 = \lambda_3 = (\alpha/(7\beta))^{1/2}$ . For the first solution a 4-fold degenerate Van Hove level splits into two doubly degenerate levels, for the second one the Van Hove level splits into one 3-fold degenerate level and one single level. The first solution has lower free energy, hence the only option at  $\gamma = \beta' = 0$  is 2-2 splitting.

For a generic case when  $\gamma$  and  $\beta'$  are non-zero, we subtract Eq. (S7) for  $l = 2$  from that for  $l = 1$  and obtain

$$0 = (\lambda_1 - \lambda_2) \left[ -\alpha + \gamma(\lambda_1 + \lambda_2) + \beta(\lambda_1^2 + \lambda_1\lambda_2 + \lambda_2^2) + \beta' \left( \sum_j \lambda_j^2 + \left( \sum_j \lambda_j \right)^2 \right) \right]. \quad (S8)$$

We see that either  $\lambda_1 = \lambda_2$  or the  $\lambda$ 's have to satisfy the quadratic equation in square brackets in (S8). Below we search for the solutions of (S7) with the constraint  $\lambda_1 = \lambda_2$ . It is straightforward to verify that enforcing instead the condition set by the quadratic equation in (S8) ultimately leads to the same solutions with permuted  $\lambda_j$ .

Let us label  $\lambda_1 = \lambda_2 = \lambda$ . The remaining two equations in (S7) are

$$\begin{aligned} 0 &= 2(\lambda + \lambda_3) \left( -\alpha - 2\gamma\lambda + \beta(4\lambda^2 + 2\lambda\lambda_3 + \lambda_3^2) + 2\beta'(3\lambda^2 + \lambda_3^2 + 2\lambda\lambda_3) \right) \\ 0 &= (\lambda - \lambda_3) \left( -\alpha + \gamma(\lambda + \lambda_3) + \beta(\lambda^2 + \lambda\lambda_3 + \lambda_3^2) + 2\beta'(3\lambda^2 + \lambda_3^2 + 2\lambda\lambda_3) \right) \end{aligned} \quad (S9)$$

The upper equation follows from (S7) for  $l = 3$  and the lower one is obtained by subtracting the equation for  $l = 3$  from that for  $l = 1$ . There are three possible solutions of these equations: (i)  $\lambda = \lambda_3$ , where  $\lambda$  is determined by the second bracket in the first equation; (ii)  $\lambda = -\lambda_3$ , where  $\lambda$  is determined by the second bracket in the second equation; (iii)  $\lambda$  and  $\lambda_3$  are different and are determined by second brackets in both equations. Let us consider those conditions one by one.

(i)  $\lambda = \lambda_3$ . Solving for  $\lambda$ , we obtain

$$\lambda = \frac{\gamma + \sqrt{\gamma^2 + \alpha(7\beta + 12\beta')}}{7\beta + 12\beta'} \quad (S10)$$

The free energy at the minimum is given by

$$\mathcal{F} = \frac{\alpha^2}{\beta} f_i(x, y), \quad (S11)$$

where  $x = \frac{\gamma}{\sqrt{\alpha\beta}}$ ,  $y = \beta'/\beta$ , and

$$f_i(x, y) = - \frac{(x + \sqrt{7 + x^2 + 12y})^2 \left[ 3(7 + 12y) + 2x(x + \sqrt{7 + x^2 + 12y}) \right]}{(7 + 12y)^3}. \quad (S12)$$

If  $\gamma < 0$ , the solution with a minus sign in front of the square roots in Eqs. (S10)+(S12) corresponds to a minimum.

(ii)  $\lambda = -\lambda_3$ . In this case

$$\lambda = \sqrt{\frac{\alpha}{\beta(1 + 4y)}}, \quad (S13)$$

and

$$\mathcal{F} = \frac{\alpha^2}{\beta} f_{ii}(x, y). \quad (S14)$$

where

$$f_{ii}(x, y) = -\frac{1}{1 + 4y} \quad (S15)$$

Note that  $f_{ii}$  is independent of  $x$ .

(iii)  $\lambda$  and  $\lambda_3$  are determined by the two quadratic equations:

$$\begin{aligned} 0 &= -\alpha + \gamma(\lambda + \lambda_3) + \beta(\lambda^2 + \lambda\lambda_3 + \lambda_3^2) + 2\beta'(3\lambda^2 + \lambda_3^2 + 2\lambda\lambda_3) \\ 0 &= -\alpha - 2\gamma\lambda + \beta(4\lambda^2 + 2\lambda\lambda_3 + \lambda_3^2) + 2\beta'(3\lambda^2 + \lambda_3^2 + 2\lambda\lambda_3) \end{aligned} \quad (S16)$$

Subtracting one from the other we obtain

$$(3\lambda + \lambda_3)(\gamma - \beta\lambda) = 0. \quad (S17)$$

The solution  $\lambda_3 = -3\lambda$  brings us back to case (i). The other solution is

$$\begin{aligned} \lambda &= \frac{\gamma}{\beta} \\ \lambda_3 &= -\frac{\gamma}{\beta} \pm \sqrt{\frac{\frac{\alpha}{\beta} - \frac{\gamma^2}{\beta^2} \left( 1 + 4\frac{\beta'}{\beta} \right)}{1 + 2\frac{\beta'}{\beta}}} \end{aligned} \quad (S18)$$

This solution exists only for  $|x| \leq 1/\sqrt{1+4y}$ . The corresponding free energy is

$$\mathcal{F} = \frac{\alpha^2}{\beta} f_{iii}(x, y) \quad (\text{S19})$$

where

$$f_{iii}(x, y) = -\frac{1 + 2x^2 - x^4(1 + 4y)}{2(1 + 2y)} \quad (\text{S20})$$

Note that the free energy is the same for both signs in front of the square root in Eq. (S18).

The solution (iii) merges with the solution (ii) at  $|x| = 1/\sqrt{1+4y}$ , where  $\lambda_3 = -\lambda$  and with the solution (i) at a smaller  $|x| = 1/\sqrt{5+12y}$  where  $\lambda_3 = \lambda$  or  $-3\lambda$ , depending on the sign in front of the square root in (S18).

We plot  $f_l(x, y)$  ( $l = i, ii, iii$ ) in Fig. 2 of the main text as function of  $x$  for  $y = 0$  and  $y = 1$ . In both cases, for large  $x$  (small positive  $\alpha$  at a non-zero  $\gamma$ ), the smallest free energy is for the state (i), and for small  $x$  (small  $\gamma$  and a finite  $\alpha$ ) the smallest free energy is for the state (ii). The intermediate state (iii) is never a minimum of  $\mathcal{F}$ . This means that there is a direct first-order transition between states (i) and (ii) at some critical  $x_{cr}$ . This result holds for all  $y$ . Still,  $f_{iii}(x, y)$  is close to  $f_i(x, y)$  and  $f_{ii}(x, y)$  near where they become equal, particularly at large  $y$ . It is then entirely possible that  $f_{iii}$  becomes the ground state near  $x_{cr}$  if we move the system away from SU(4) symmetry by, e.g., adding interaction terms which scatter between valleys. In this case the transition from state (i) at large  $x$  to state (ii) at small  $x$  becomes a continuous one via an intermediate phase.

### B. Symmetry properties

(i)  $\lambda = \lambda_3$ . In the diagonal basis, the matrix  $\hat{\Phi}$  is

$$\hat{\Phi} = \text{diag}(\lambda, \lambda, \lambda, -3\lambda), \quad (\text{S21})$$

The remnant symmetry of this state is  $SU(3) \times U(1)$ , which is a subgroup of the original SU(4) symmetry group. Here, SU(3) corresponds to symmetry transformations in the subspace of the first three components of  $\hat{\Phi}$  and U(1) to a relative phase variation between the last and the first three components. Up to rotations of the overall phase, the SU(3) and U(1) generators are given by block-diagonal matrices

$$U_{SU(3)} = \text{diag}(e^{i\alpha_i T^i}, 1), \quad U_{U(1)} = \text{diag}(\mathbb{1}_3, e^{i\theta}) \quad (\text{S22})$$

where  $T^i$ ,  $i = 1, \dots, 8$  are eight Gell-Mann matrices, and  $\mathbb{1}$  is a  $3 \times 3$  identity matrix.

(ii)  $\lambda = -\lambda_3$ . The matrix  $\hat{\Phi}$  is

$$\hat{\Phi} = \text{diag}(\lambda, \lambda, -\lambda, -\lambda) \quad (\text{S23})$$

The remnant symmetry of this state is  $SU(2) \times SU(2) \times U(1)$ , where the two SU(2)'s correspond to rotations within the subsets of the first two and the last two components of  $\hat{\Phi}$ , and U(1) corresponds to a rotation of one subset relative to the other. They can be represented by

$$\begin{aligned} U_{SU(2)} &= \text{diag}(e^{i\alpha_i \sigma^i}, \mathbb{1}_2) \\ U'_{SU(2)} &= \text{diag}(\mathbb{1}_2, e^{i\alpha_i \sigma^i}) \\ U_{U(1)} &= \text{diag}(\mathbb{1}_2, e^{i\theta} \mathbb{1}_2), \end{aligned} \quad (\text{S24})$$

where  $\sigma^i$  are the Pauli matrices.

(iii)  $\lambda \neq \pm\lambda_3$ . The matrix  $\hat{\Phi}$  is

$$\text{diag}(\lambda, \lambda, -\lambda_3, -2\lambda + \lambda_3) \quad (\text{S25})$$

The remnant symmetry of this state is  $SU(2) \times U(1) \times U(1)$ , where SU(2) correspond to rotations within the subsets of the first two components and the two U(1)'s corresponds to independent, relative rotations of the third and the fourth components, e.g.,

$$\begin{aligned} U_{SU(2)} &= \text{diag}(e^{i\alpha_i \sigma^i}, \mathbb{1}_2) \\ U_{U(1)} &= \text{diag}(\mathbb{1}_2, e^{i\theta}, 1) \\ U'_{U(1)} &= \text{diag}(\mathbb{1}_2, 1, e^{i\theta}). \end{aligned} \quad (\text{S26})$$

### C. Relaxing SU(4) symmetry

As we mentioned at the beginning, the 15 order parameters with near-equal, attractive couplings near Van Hove filling consist of two subsets with seven intra-valley,  $Q = 0$  order parameters and eight inter-valley,  $Q \neq 0$  order parameters. The set with seven order parameters is described by the order parameter matrix  $\hat{\Phi}_7 = \sum \varphi_{ij}^{(7)} \sigma_i \tau_j$  with  $i = 0, \dots, 3$ ,  $j = 0, 3$ , excluding  $i = j = 0$ , and  $\sigma_i$  ( $\tau_j$ ) are Pauli matrices for (iso-)spin degrees of freedom, where  $\sigma_0 = \tau_0 = \mathbb{1}_2$ . The set with eight order parameters is described by  $\hat{\Phi}_8 = \sum \varphi_{ij}^{(8)} \sigma_i \tau_j$  with  $i = 0, \dots, 3$  and  $j = 1, 2$  [23]. There is a single coupling constant within each set ( $\lambda_7$  and  $\lambda_8$ , respectively). In the microscopic model that we used to derive the free energy,  $\lambda_7$  and  $\lambda_8$  are close in magnitude. In our analysis above, we neglected the difference between these two couplings, in which case the free energy is SU(4)-symmetric.

Here we briefly analyze what happens if we do not treat  $\lambda_7$  and  $\lambda_8$  as equal and instead assume that one of the two is larger and the order is formed within either the set of 7 or the set of 8. Keeping only one of the sets, integrating out fermion fields, and approximating the bare Green's functions for all spins and isospins to be equal, we obtain again the free energy in the form

$$\mathcal{F}_\mu = -\frac{\alpha}{2} \text{Tr}[\hat{\Phi}_\mu^2] + \frac{\gamma}{3} \text{Tr}[\hat{\Phi}_\mu^3] + \frac{\beta}{4} \text{Tr}[\hat{\Phi}_\mu^4] \quad (\text{S27})$$

with  $\mu = 7, 8$ . Here we neglect any symmetry-allowed terms that are not produced by integrating out the fermions and appear as higher-order effects.

Diagonalization of  $\hat{\Phi}_\mu$  shows that

$$\hat{\Phi}_7 \sim \text{diag}[\lambda_1, \lambda_2, \lambda_3, -(\lambda_1 + \lambda_2 + \lambda_3)] \quad (\text{S28})$$

$$\hat{\Phi}_8 \sim \text{diag}[\lambda_1, -\lambda_1, \lambda_2, -\lambda_2]. \quad (\text{S29})$$

Using this in Eq. (S27), we obtain for  $\mathcal{F}_7$  the same expression as in the SU(4) symmetric case. Thus, within the set of 7 intra-valley  $Q = 0$  order parameters one obtains the same ordered states as in SU(4)-symmetric model, and hence the same sequence of splittings of VH peak components (1-3 (3-1) and 2-2) and the same cascade of transitions. For the set of 8 inter-valley order parameters  $\text{Tr}[\hat{\Phi}_\mu^3]$  vanishes. Then the ordered state gives rise to only  $2 - 2'$  splitting of VH peaks. There is no phases with 1-3 (3-1) splitting and, hence, no cascade of transitions.

#### D. The ground state of an SU(3)-symmetric free energy

We next consider the case of an SU(3)-symmetric free energy. Such a symmetry of fermionic bilinears can emerge when there are three degenerate bands near Van Hove points (this is the case when the dispersion of one of the initially 4 degenerate bands shifts such that the whole band moves away from the chemical potential). Like we said, for the  $N = 3$  case one can set  $\beta' = 0$  without losing generality.

In the SU(3)-symmetric case the order parameter matrix reads

$$\hat{\Phi} = \text{diag}(\lambda_1, \lambda_2, -(\lambda_1 + \lambda_2)) \quad (\text{S30})$$

and the conditions for extrema are

$$-\alpha(2\lambda_1 + \lambda_2) + \gamma(\lambda_1^2 - (\lambda_1 + \lambda_2)^2) + \beta(\lambda_1^3 + (\lambda_1 + \lambda_2)^3) = 0, \quad (\text{S31})$$

$$-\alpha(2\lambda_2 + \lambda_1) + \gamma(\lambda_2^2 - (\lambda_1 + \lambda_2)^2) + \beta(\lambda_2^3 + (\lambda_1 + \lambda_2)^3) = 0. \quad (\text{S32})$$

Subtracting one equation from the other, we obtain that either  $\lambda_1 = \lambda_2$ , or  $-\alpha - \gamma(\lambda_1 + \lambda_2) + \beta(\lambda_1^2 + \lambda_2^2 + \lambda_1\lambda_2) = 0$ . In the first case,  $\hat{\Phi} = \text{diag}(\lambda, \lambda, -2\lambda)$ , where

$$\lambda = \frac{\gamma \pm \sqrt{12\alpha\beta + \gamma^2}}{6\beta}. \quad (\text{S33})$$

The free energy is

$$F = -\frac{\alpha^2}{\beta} g(x), \quad (\text{S34})$$

with

$$g(x) = \frac{(x \pm \sqrt{12 + x^2})^2 (18 + x(x \pm \sqrt{12 + x^2}))}{432}. \quad (\text{S35})$$

The choice of  $\pm$  in (S33),(S35) depends on the sign of  $\gamma$ .

We analyzed the second condition,  $-\alpha - \gamma(\lambda_1 + \lambda_2) + \beta(\lambda_1^2 + \lambda_2^2 + \lambda_1\lambda_2) = 0$ , and found that it yields  $\lambda_2 = -2\lambda_1$ , i.e.,  $\hat{\Phi} = \text{diag}(\lambda, -2\lambda, \lambda)$ . This is the same  $\hat{\Phi}'$  as above, up to permutations of the components. Accordingly,  $\lambda$  and the free energy are the same as in (S35).

We argue therefore that in the SU(3) model the ordered state is the same for all  $|x|$ . This is the key distinction from the SU(4) model, where the ordered state changes between large and small  $|x|$ .

The remnant symmetry of the system in the ordered state is SU(2)  $\times$  U(1). Here, SU(2) corresponds to symmetry transformations for the first two components of  $\hat{\Phi} = \text{diag}(\lambda, \lambda, -2\lambda)$  and U(1) corresponds to a relative phase variation between the first two and the last components.

## S2. DERIVATION OF SU(3)-SYMMETRIC LANDAU FUNCTIONAL FROM THE MICROSCOPIC MODEL

### A. 6-patch model

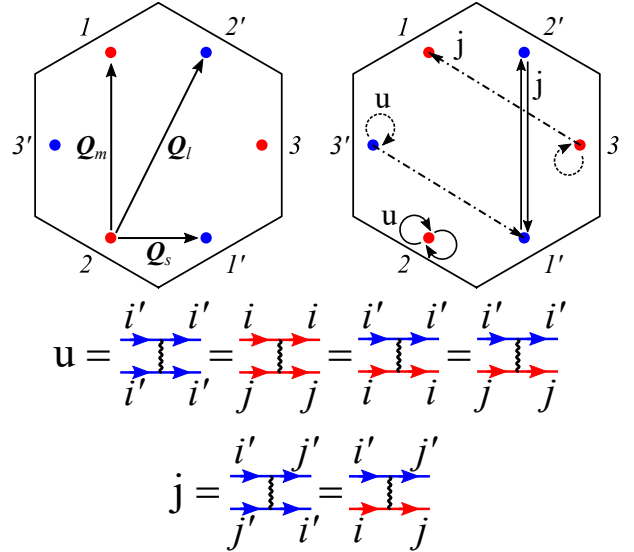


FIG. S1. Left: The sketch of a 6-patch model. Circles indicate the location of patches and color indicates valley composition. We assume that the blue valley is “spinless”. Vectors  $\mathbf{Q}_s, \mathbf{Q}_m, \mathbf{Q}_l$  connect patches in momentum space. Right: sketch of interactions between patch fermions. The couplings are shown below.

Here we show how the SU(3) symmetry appears in the 6-patch model in the case of one valley hosting electrons with only one spin projection. The sketch of patch structure, momentum transfer vectors, and interactions is given in Fig. S1. Density-density interactions between each patch are identical, exchange interaction is allowed if fermions do

not change their valley in the process of scattering. The coupling constants and polarization operators are the same as in the full 6-patch model with VH singularities of all 4 bands at the Fermi level. Every patch in the model we consider here is valley-polarized and one of the valleys is also spin-polarized. We label patches by  $i = 1, 2, 3$  for valley + and by  $i' = 1, 2, 3$  for valley -, spins by  $s, s' = \uparrow, \downarrow$  and consider valley - as spinless, i.e., having only one spin projection. For the interaction we use the same model as in Ref. [22] with density-density and exchange couplings  $u$  and  $j$ .

We introduce all possible order parameters involving fermions near VH points:

$$\begin{aligned}
\Delta_{Pom,+i}^c &= \langle f_{+,s,i}^\dagger \delta_{ss'} f_{+,s',i} \rangle, \\
\Delta_{Pom,+i}^s &= \langle f_{+,s,i}^\dagger \sigma_{ss'} f_{+,s',i} \rangle, \\
\Delta_{Pom,-i'} &= \langle f_{-,i'}^\dagger f_{-,i'} \rangle, \\
\Delta_{Q_s,+,-,\uparrow,i} &= \langle f_{+,\uparrow,(i+2)}^\dagger f_{-, (i+1)'} \rangle, \\
\Delta_{Q_s,+,-,\uparrow,i'} &= \langle f_{+,\uparrow,(i+1)}^\dagger f_{-, (i+2)'} \rangle, \\
\Delta_{Q_s,+,-,\downarrow,i} &= \langle f_{+,\downarrow,(i+2)}^\dagger f_{-, (i+1)'} \rangle \\
\Delta_{Q_s,+,-,\downarrow,i'} &= \langle f_{+,\downarrow,(i+1)}^\dagger f_{-, (i+2)'} \rangle \\
\Delta_{Q_m,+i}^c &= \langle f_{+,s,i+2}^\dagger \delta_{ss'} f_{+,s',i+1} \rangle, \\
\Delta_{Q_m,+i}^s &= \langle f_{+,s,i+2}^\dagger \sigma_{ss'} f_{+,s',i+1} \rangle, \\
\Delta_{Q_m,-i'} &= \langle f_{-, (i+2)'}^\dagger f_{-, (i+1)'} \rangle, \\
\Delta_{Q_l,+,-,\uparrow,i} &= \langle f_{+,\uparrow,i}^\dagger f_{-,i'} \rangle, \\
\Delta_{Q_l,+,-,\downarrow,i} &= \langle f_{+,\downarrow,i}^\dagger f_{-,i'} \rangle.
\end{aligned} \tag{S36}$$

There are also conjugated parameters, which we omitted for brevity.

We first consider intra-valley  $Q = 0$  channels. There are six charge order parameters:

$$\Gamma(Q = 0)^c = (\Delta_{Pom,+1}^c \Delta_{Pom,+2}^c \Delta_{Pom,+3}^c \Delta_{Pom,-,1'} \Delta_{Pom,-,2'} \Delta_{Pom,-,3'}).$$

As usual, we assume that bare order parameters are infinitesimally small and dress them by the interactions in the ladder approximation. We obtain

$$\Gamma(Q = 0)^c = \Gamma(Q = 0)^{c,(0)} + \Pi(0) \Lambda_{Q=0}^c \Gamma(Q = 0)^c, \tag{S37}$$

where  $\Pi(0)$  is the polarization operator,  $\Gamma(Q = 0)^{c,(0)}$  is bare (infinitesimal) order parameter, and  $\Gamma(Q = 0)^c$  is the dressed order parameter. The matrix  $\Lambda_{Q=0}^c$  has the form

$$\Lambda_{Q=0}^c = \begin{pmatrix} -u & j-2u & j-2u & -u & -u & -u \\ j-2u & -u & j-2u & -u & -u & -u \\ j-2u & j-2u & -u & -u & -u & -u \\ -2u & -2u & -2u & 0 & j-u & j-u \\ -2u & -2u & -2u & j-u & 0 & j-u \\ -2u & -2u & -2u & j-u & j-u & 0 \end{pmatrix}. \tag{S38}$$

The largest eigenvalue of this matrix is  $\lambda_{Pom}^{c,s^\pm} = u + 2j$  and the corresponding eigenvector is  $(-\frac{1}{2}, -\frac{1}{2}, -\frac{1}{2}, 1, 1, 1)$ . It describes  $s^\pm$ -wave charge Pomeranchuk order, which is symmetric with respect to 3 VH points from the same valley and changes sign between valleys. This order leads to valley polarization.

A  $Q = 0$  spin order parameter can only be introduced for the spinfull valley, therefore

$$\Gamma(Q = 0)^s = (\Delta_{Pom,+1}^s \Delta_{Pom,+2}^s \Delta_{Pom,+3}^s)$$

with the coupling matrix

$$\Lambda_{Q=0}^s = \begin{pmatrix} u & j & j \\ j & u & j \\ j & j & u \end{pmatrix}. \tag{S39}$$

The largest eigenvalue is again  $u + 2j$ . The corresponding eigenvector is  $(1, 1, 1)$ , i.e., this order is again  $s$ -wave with respect to three VH points from the same valley.

Now consider intra-valley density wave orders. In general, such an order can be with any momenta connecting VH points. Intra-valley density-wave orders are with momenta  $Q_m$  and inter-valley density-wave orders are with  $Q_l$  and  $Q_s$  (see Fig. S1).

We begin with intra-valley orders. As for  $Q = 0$ , the order in the spin channel can be only introduced for the spinfull valley +. The corresponding order parameters are

$$\Gamma(Q_m)^s = (\Delta_{Q_m,+1}^s \Delta_{Q_m,+2}^s \Delta_{Q_m,+3}^s)$$

and the coupling matrix is

$$\Lambda_{Q_m}^s = u \mathbb{1}_{3 \times 3} \tag{S40}$$

with three eigenvalues equal to  $u$ . The charge channel is more interesting. Here

$$\Gamma(Q_m)^c = (\Delta_{Q_m,+1}^c \Delta_{Q_m,+2}^c \Delta_{Q_m,+3}^c \bar{\Delta}_{Q_m,-,1'} \bar{\Delta}_{Q_m,-,2'} \bar{\Delta}_{Q_m,-,3'}),$$

where  $\bar{\Delta}$  is a conjugate of  $\Delta$ . The matrix of the couplings is

$$\Lambda_{Q_m}^c = \begin{pmatrix} u-2j & 0 & 0 & -j & 0 & 0 \\ 0 & u-2j & 0 & 0 & -j & 0 \\ 0 & 0 & u-2j & 0 & 0 & -j \\ -2j & 0 & 0 & u-j & 0 & 0 \\ 0 & -2j & 0 & 0 & u-j & 0 \\ 0 & 0 & -2j & 0 & 0 & u-j \end{pmatrix}. \tag{S41}$$

The two eigenvalues of this matrix are  $u$  and  $u - 3j$ .

Now we proceed to inter-valley orders. Note, that for inter-valley orders the spin/charge dichotomy does not work anymore. Consider first the orders with momentum  $Q_l$ . The order parameters are

$$\Gamma(Q_l) =$$

$$(\Delta_{Q_l,+,-,\uparrow,1} \Delta_{Q_l,+,-,\uparrow,2} \Delta_{Q_l,+,-,\uparrow,3} \Delta_{Q_l,+,-,\downarrow,1} \Delta_{Q_l,+,-,\downarrow,2} \Delta_{Q_l,+,-,\downarrow,3}). \tag{S42}$$

The coupling matrix is diagonal

$$\Lambda_{\mathcal{Q}_s}^s = u \mathbb{1}_{6 \times 6} \quad (\text{S43})$$

and has identical eigenvalues  $u$ .

We now consider inter-valley orders with momentum  $\mathcal{Q}_s$ . The corresponding order parameters are

$$\Gamma(\mathcal{Q}_s) = (\Delta_{\mathcal{Q}_s,+-,\uparrow,1} \Delta_{\mathcal{Q}_s,+-,\uparrow,2} \Delta_{\mathcal{Q}_s,+-,\uparrow,3} \Delta_{\mathcal{Q}_s,+-,\uparrow,1'} \Delta_{\mathcal{Q}_s,+-,\uparrow,2'} \Delta_{\mathcal{Q}_s,+-,\uparrow,3'}). \quad (\text{S44})$$

The coupling matrix is

$$\Lambda_{\mathcal{Q}_s} = \begin{pmatrix} u & 0 & 0 & j & 0 & 0 \\ 0 & u & 0 & 0 & j & 0 \\ 0 & 0 & u & 0 & 0 & j \\ j & 0 & 0 & u & 0 & 0 \\ 0 & j & 0 & 0 & u & 0 \\ 0 & 0 & j & 0 & 0 & u \end{pmatrix}. \quad (\text{S45})$$

The leading eigenvalue here is  $u + j$ . It again corresponds to  $s$ -wave order, symmetric with respect to three VH points from the same valley (or, equivalently, symmetric with respect to three possible  $\mathcal{Q}_s$  between neighboring VH points from different valleys). Evaluating the products of the eigenvalues and the polarizations to obtain dimensionless couplings and comparing different channels, we find that  $s$ -wave  $\mathcal{Q} = 0$  channel and  $s$ -wave  $\mathcal{Q}_s$  channel are almost degenerate. This is the same type of degeneracy as in the model with spinfull fermions [22].

The outcome of this analysis is that there are 8 almost degenerate order parameters: one scalar intra-valley charge  $\mathcal{Q} = 0$  order parameter, one 3-component intra-valley  $\mathcal{Q} = 0$  vector spin order parameter, and four inter-valley order parameters with momenta  $\mathcal{Q}_s$ , which one can treat as 4 scalars. These 8 order parameters form an adjoint representation of SU(3).

The matrix Green's function, symmetric with respect to 3 VH points from the same valley, is a  $3 \times 3$  matrix in band space. The Green's function of free fermions is diagonal and isotropic:

$$\hat{G}_0 = \begin{pmatrix} G & 0 & 0 \\ 0 & G & 0 \\ 0 & 0 & G \end{pmatrix}, \quad (\text{S46})$$

where  $G^{-1} = i\omega_m - \xi_k$  with Matsubara frequency  $\omega_m$  and fermion dispersion  $\xi_k$ . We associate the bottom component with the spinless valley. Once the order sets in, the Green's function gets modified. It is convenient to introduce the valley polarization order parameter  $\phi$  via

$$\Delta_{\mathcal{P}om,+}^c = \frac{1}{\sqrt{3}}\phi, \quad \Delta_{\mathcal{P}om,-} = -\frac{2}{\sqrt{3}}\phi, \quad (\text{S47})$$

and introduce inter-valley order parameters  $S_{A1}, S_{A2}, S_{B1}, S_{B2}$  related to the magnitudes of inter-valley order parameters (identical for 3 directions of

vectors  $\mathcal{Q}_s$ )  $\Delta_{\mathcal{Q}_s,+-,\uparrow}, \Delta_{\mathcal{Q}_s,+-,\downarrow}$  and their conjugated  $\bar{\Delta}_{\mathcal{Q}_s,+-,\uparrow}$  and  $\bar{\Delta}_{\mathcal{Q}_s,+-,\downarrow}$  via

$$\begin{aligned} S_{A2} - iS_{B2} &= \Delta_{\mathcal{Q}_s,+-,\uparrow}, \quad S_{A1} - iS_{B1} = \Delta_{\mathcal{Q}_s,+-,\downarrow}, \\ S_{A2} + iS_{B2} &= \bar{\Delta}_{\mathcal{Q}_s,+-,\uparrow}, \quad S_{A1} + iS_{B1} = \bar{\Delta}_{\mathcal{Q}_s,+-,\downarrow}, \end{aligned} \quad (\text{S48})$$

We label the three-component vector spin intra-valley order parameter  $\Delta_{\mathcal{P}om,+}^s$  as just  $\mathbf{S}$ .

In matrix notations we then have  $\hat{G} = \hat{G}_0 + \hat{\phi} + \hat{S} + \hat{S}_{AB}$ , where

$$\begin{aligned} \hat{\phi} &= \frac{1}{\sqrt{3}} \begin{pmatrix} \phi & 0 & 0 \\ 0 & \phi & 0 \\ 0 & 0 & -2\phi \end{pmatrix}, \\ \hat{S} &= \begin{pmatrix} S_z & S_x - iS_y & 0 \\ S_x + iS_y & -S_z & 0 \\ 0 & 0 & 0 \end{pmatrix}, \\ \hat{S}_{AB} &= \begin{pmatrix} 0 & 0 & S_{A2} - iS_{B2} \\ 0 & 0 & S_{A1} - iS_{B1} \\ S_{A2} + iS_{B2} & S_{A1} + iS_{B1} & 0 \end{pmatrix}. \end{aligned} \quad (\text{S49})$$

Expressed via the standard form of Gell-Mann matrices,  $\hat{\phi}$  corresponds to matrix  $T^8$ ,  $\hat{S}$  corresponds to  $T^1, T^2, T^3$ , and  $\hat{S}_{AB}$  corresponds to  $T^4, T^5, T^6, T^7$ , where  $T^i$  with  $i = 1 \dots 8$  are the eight generators of the group SU(3).

## B. The ground state of the SU(3) model in terms of fermionic bilinears

The ordered state in the SU(3) model can be straightforwardly expressed via fermionic bilinears. For simplicity, we present the result for the case when inter-valley components  $S_{A1}, S_{A2}$  and  $S_{B1}, S_{B2}$  are absent and the order is specified by  $\phi$  and  $\mathbf{S}$ . The same free energy as in (S35), expressed in terms of  $\phi$  and  $\mathbf{S}$  is

$$F = \alpha(\phi^2 + \mathbf{S} \cdot \mathbf{S}) + \frac{2\gamma}{\sqrt{3}}\phi(\mathbf{S} \cdot \mathbf{S} - \frac{\phi^2}{3}) + \frac{\beta}{2}(\phi^2 + \mathbf{S} \cdot \mathbf{S})^2 \quad (\text{S50})$$

We introduce a standard parameterization for magnitudes of order parameters:  $|\mathbf{S}| = r \cos \theta$ ,  $\phi = r \sin \theta$  and rewrite the free energy in the form

$$F = \alpha r^2 + \frac{2\gamma}{3\sqrt{3}}r^3 \sin 3\theta + \frac{\beta}{2}r^4. \quad (\text{S51})$$

The ground state is reached when  $\sin 3\theta = -1$ , i.e., for  $\theta = \frac{\pi}{2}, \frac{7\pi}{6}, \frac{11\pi}{6}$ . The ordered states, which we earlier specified by  $\hat{\Phi} = (\lambda, \lambda, -2\lambda)$  (up to permutations) with  $\lambda$  given by Eq. (S33), are expressed in terms of  $\phi$  and  $\mathbf{S}$  as

$$\begin{aligned} \phi &= r, |\mathbf{S}| = 0, \\ \phi &= -\frac{r}{2}, |\mathbf{S}| = -\frac{r\sqrt{3}}{2}, \\ \phi &= -\frac{r}{2}, |\mathbf{S}| = \frac{r\sqrt{3}}{2}. \end{aligned} \quad (\text{S52})$$

The first state is a pure valley order, for which the two-fold degeneracy stems from the unbroken spin degeneracy of the spinfull valley. The other two states correspond to mixed spin-valley order. There, the degenerate levels necessarily belong to different valleys, however, spin directions remain degenerate.

### S3. ANOTHER SCENARIO FOR THE CASCADE OF TRANSITIONS

Here we discuss another scenario for the cascade, in which the component of the Van Hove peak that crosses the Fermi level, no longer contributes to particle-hole order. This scenario is qualitatively similar to the one put forward in Ref. [15], in which one of the bands gets fully filled (fully depleted) at each transition from the cascade and after that does not contribute to particle-hole order, and to the one in Ref. [14], in which a flat band gets severely broadened after crossing the Fermi level. We do not assume full filling/full depletion or strong broadening, but still exercise here the idea that one of the bands effectively disappears after each transition, and the symmetry of the Landau free energy progressively reduces from  $SU(4)$  to  $SU(3)$  and then to  $SU(2)$ . In this scenario the pattern of symmetry changes at the transitions from the cascade is

$$\begin{aligned} n \approx 1 : & \quad SU(4) \rightarrow SU(3) \times U(1) \\ n \approx 2 : & \quad SU(3) \rightarrow SU(2) \times U(1) \\ n \approx 3 : & \quad SU(2) \rightarrow U(1). \end{aligned} \quad (S53)$$

and the number of relevant bands that contribute to particle-hole orders changes from 4 to 3 at  $|n| \approx 1$ , from 3 to 2 at  $|n| \approx 2$ , and from 2 to 1 at  $|n| \approx 3$ .

The first transition and the manifold of the ordered states is exactly the same as in the  $SU(4)$  model from the main text, and the splitting of the VH peak is 3-1, with one component crossing the Fermi level. At the second transition, one component of 3-fold degenerate VH peak crosses the Fermi level. The manifold of the ordered states is the same as in the 2-2 phase of the  $SU(4)$  model.

For the last transition, the relevant model contains either two spinless fermions from different valleys or one valley with both spin projections. In either case the system obeys  $SU(2)$  symmetry: in valley space in the former and in spin space in the latter. For the valley  $SU(2)$  case the only particle-hole order parameter is charge valley polarization. Interaction for this order parameter is attractive, and gives rise to an instability that moves one VH peak component through the Fermi level and splits the doubly degenerate VH peak into 1-1. For the spin  $SU(2)$  case the only instability is the standard Stoner-like ferromagnetism that leads to the splitting of two levels. Finally, as  $|n|$  comes close to 4, the last VH peak component moves through the Fermi level.

Note that the first two transitions, near  $|n| = 1$  and  $|n| = 2$ , are first order, the one near  $|n| = 3$  is second order, and the last crossing near  $|n| = 4$  is continuous in our present description, but may actually also involve a phase transition, as we argue in the next subsection.

Within this scenario, one can naturally explain the emergence of insulating states at integer fillings, but it is a priori unclear how the peak components which are assumed to be at different energies as they cross the Fermi level at different  $n$ , recombine back into a 4-fold degenerate strong VH peak once the order disappears at  $|n| \lesssim 4$ .

#### A. Instability of spinless fermions from a single valley

Above we considered VH points that are related by  $C_3$  lattice rotational symmetry and assumed that magnitudes of order parameter are identical on every patch. Here we relax this assumption and check if other particle-hole orders are possible. This issue is most relevant for the case of spinless fermions near 3 VH points in only one valley i.e., the case near  $|n| \lesssim 4$  when only one fermion species from a single valley remains.

We label the fermions from the three VH points as  $f_i$ ,  $i = 1, 2, 3$ , see Fig. S2. Because fermions are spinless, only charge orders are possible. There are two potential orders: the one with  $Q = 0$  and the one with  $Q$  between Van Hove points. Each order parameter has three components. The

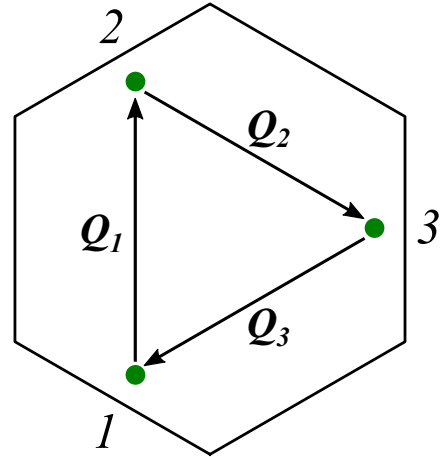


FIG. S2. The sketch of a patch model for a band with only one occupied valley. Green circles indicate the location of Van Hove points. Three vectors indicate the directions of momentum transfer between each pair of patches. This is the momentum transfer of the density wave.

order parameters are

$$\begin{aligned}\Delta_{Pom,i} &= \langle f_i^\dagger f_i \rangle, \\ \Delta_{Q_i} &= \langle f_{i+1}^\dagger f_i \rangle.\end{aligned}\tag{S54}$$

Like in Sec. S2 we consider density-density and exchange interactions ( $u$  and  $j$  terms, respectively). In the ladder approximation the two order parameters do not couple and can be considered independent of each other. For the three  $Q = 0$  order parameters the coupling matrix is

$$\Lambda_{Q=0} = \begin{pmatrix} 0 & j-u & j-u \\ j-u & 0 & j-u \\ j-u & j-u & 0 \end{pmatrix}\tag{S55}$$

There are three eigenvalues:  $\lambda^s = 2(j-u)$ , which corresponds to an  $s$ -wave order parameter with eigenvector  $(1, 1, 1)$ , and two-fold degenerate  $\lambda^d = u-j$ , with  $d$ -wave eigenvectors  $(-1, 0, 1)$  and  $(1/2, -1, 1/2)$ . For  $u > j$ , as expected on general grounds,  $\lambda^d$  is positive (attractive) and  $\lambda^s$

is negative (repulsive). If the  $s$ -wave  $Q = 0$  order parameter is imposed, the VH peak crosses the Fermi level without inducing a particle-hole order.

For finite  $Q$  orders, the coupling matrix is

$$\Lambda_Q = \begin{pmatrix} u-j & 0 & 0 \\ 0 & u-j & 0 \\ 0 & 0 & u-j \end{pmatrix}.\tag{S56}$$

We see that the eigenfunctions for all three combinations of  $\Delta_{Q_i}$  (one is  $s$ -wave and two are  $d$ -wave) are identical and the same as for the  $d$ -wave  $Q = 0$  order parameter. The polarization operator for  $Q = 0$  is slightly larger than the one with finite  $Q$  (Ref. [22]). Hence  $d$ -wave  $Q = 0$  order is the most likely one. Such an order splits the energies of the three VH peaks. So far, no clear evidence for such order has been reported, see however, Ref. 45. One option may be that such order oscillates between the two  $d$ -wave components at short spatial scales, and on average all three VH peaks move identically, like if there was no particle-hole order.